Cancer Letters 527 (2022) 150–163

Contents lists available at ScienceDirect

Cancer Letters

journal homepage: www.elsevier.com/locate/canlet

Original Articles

SETD8 stabilized by USP17 epigenetically activates SREBP1 pathway to drive lipogenesis and oncogenesis of ccRCC

Xiaofeng Li [a,b], Zhengfang Liu [a], Chuanyou Xia [c], Keqiang Yan [a], Zhiqing Fang [a,**], Yidong Fan [a,*]

[a] Department of Urology, Qilu Hospital, Cheeloo College of Medicine, Shandong University, Ji Nan 250012, Shandong, China
[b] Key Laboratory of Cardio-vascular Remodeling and Function Research, Chinese Ministry of Education, Chinese Ministry of Health, China
[c] The First Affiliated Hospital of Shandong First Medical University/Shandong Provincial Qian-Fo-Shan Hospital, China

A B S T R A C T

Recently, epigenetic modifications, including DNA methylation, histone modification and noncoding RNA (ncRNA)-associated gene silencing, have received increasing attention from the scientific community. Many studies have demonstrated that epigenetic regulation can render dynamic alterations in the transcriptional potential of a cell, which then affects the cell's biological function. The initiation and development of clear cell renal cell carcinoma (ccRCC), the most common subtype of renal cell cancer (RCC), is also closely related to genomic alterations by epigenetic modification. For ccRCC, lipid accumulation is one of the most typical characteristics. In other words, dysregulation of lipid uptake and synthesis occurs in ccRCC, which inversely promotes cancer proliferation and progression. However, the link among epigenetic alterations, lipid biosynthesis and renal cancer progression remains unclear. SETD8 is a histone methyltransferase and plays pivotal roles in cell cycle regulation and oncogenesis of various cancers, but its role in RCC is not well understood. In this study, we discovered that SETD8 was significantly overexpressed in RCC tumors, which was positively related to lipid storage and correlated with advanced tumor grade and stage and poor patient prognosis. Depletion of SETD8 by siRNAs or inhibitor UNC0379 diminished fatty acid (FA) de novo synthesis, cell proliferation and metastasis in ccRCC cells. Mechanistically, SETD8, which was posttranslationally stabilized by USP17, could transcriptionally modulate sterol regulatory element-binding protein 1 (SREBP1), a key transcription factor in fatty acid biosynthesis and lipogenesis, by monomethylating the 20th lysine of the H4 histone, elevating lipid biosynthesis and accumulation in RCC and further promoting cancer progression and metastasis. Taken together, the USP17/SETD8/SREBP1 signaling pathway plays a pivotal role in promoting RCC progression. SETD8 might be a novel biomarker and potential therapeutic target for treating RCC.

1. Introduction

Over 400,000 new cases of renal cell carcinoma (RCC) are reported to occur worldwide, and nearly 180,000 deaths are caused by renal cell carcinoma (RCC) per year [1]. RCC has various subtypes, and approximately 75% of cases are classified as clear cell RCC (ccRCC). Many drivers of ccRCC ontogeny and development contribute to the evolution of ccRCC into a potentially lethal disease, including VHL loss of function, genomic instability and epigenetic modulation [2]. Epigenetic modifications are frequent in RCC, and important signaling pathways are epigenetically deregulated by aberrant promoter methylation of pathway components [3].

Chromatin-based events that regulate DNA-templated processes are generally described as epigenetics. Proved by a series of findings, epigenetic modifications play a critical role in the regulation of all DNA-based processes, such as transcription, DNA repair, and replication. Consequently, abnormal expression patterns or genomic alterations of chromatin regulators can have profound results and may lead to the initiation and progression of distinct cancers [4]. These DNA and histone modifications are dynamically regulated by chromatin-modifying enzymes. SETD8, also known as PR-SET7, SET8 or KMT5A, is a member of the SET domain-containing family and a unique mammalian enzyme for

; RCC, renal cell carcinoma; ccRCC, clear cell renal cell carcinoma; SETD8, SET domain containing 8, histone lysine methyltransferase; KMT5A, lysine methyltransferase 5A; SREBF1, sterol regulatory element-binding transcription factor 1; SREBP1, sterol regulatory element-binding protein 1; H4K20me1, monomethylation of histone H4 Lys20; USP17, ubiquitin-specific peptidase 17; HEK 293T, Human Embryonic Kidney 293T; TCGA, The Cancer Genome Atlas; GSEA, Gene Set Enrichment Analysis; ECL, Enhanced Chemiluminescence; IHC, immunohistochemistry; CHX, cycloheximide; CCK-8, Cell Counting Kit-8; ORO, oil Red o; ChIP, Chromatin immunoprecipitation; TMA, Tissue microarray; DUBs, Deubiquitinases; ACACA, acetyl-CoA carboxylase alpha; SCD1, Stearoyl-Coenzyme A desaturase 1; FASN, Fatty acid synthase; FA, fatty acid.

* Corresponding author. Department of Urology, Qilu Hospital of Shandong University, Ji'nan, China.
** Corresponding author. Department of Urology, Qilu Hospital of Shandong University, Ji'nan, China.
E-mail addresses: fxl2009fxl@163.com (X. Li), lzfang9159@163.com (Z. Liu), chuanyou.xia@ki.se (C. Xia), yankeqiang1@126.com (K. Yan), doctor_fangzq@sdu.edu.cn (Z. Fang), fanyd@sdu.edu.cn (Y. Fan).

https://doi.org/10.1016/j.canlet.2021.12.018
Received 3 August 2021; Received in revised form 1 December 2021; Accepted 13 December 2021
Available online 21 December 2021

catalyzing the monomethylation of histone H4 Lys20 (H4K20me1) [5]. SETD8-mediated epigenetic modifications play a crucial role in various physiological and pathological processes, such as cell cycle progression, transcriptional regulation, adipogenesis, and cancer.

Additionally, dysregulation of lipid metabolism occurs in ccRCC [6–8]. Such metabolism aberrations in ccRCC enable cancer cells to outcompete normal cells, and they show a clear survival advantage. It is generally accepted that lipid deposition is a typical characteristic of RCC. Such lipid accumulation is beneficial to cancerous cells by functioning as energy sources and providing raw materials that represent the structural basis for biological membranes and signaling molecules, which are both critical for cellular proliferation and survival. As previously mentioned, SETD8 is involved in the regulation of the lipid metabolism process, namely, adipogenesis [9]. In addition, SETD8 is also confirmed to modulate lipid metabolism in papillary thyroid cancer [10]. However, the role and functional mechanism of SETD8 in RCC remain ambiguous and poorly understood.

Membrane-bound, basic helix-loop-helix leucine zipper (bHLHLZ) transcription factors called sterol regulatory element-binding proteins (SREBPs) have been verified to play a central role in cell metabolism by regulating the synthesis of fatty acids, triglycerides and cholesterol [11]. SREBP1 encoded by SREBF1 is involved in fatty acid and cholesterol synthesis, and it controls cellular lipogenesis and maintains lipid homeostasis, which are essential for cell viability. Multiple studies have demonstrated that SREBP1 plays central roles in promoting the progression of various cancers, such as pancreatic cancer [12], breast cancer [13], prostate cancer [14], and colon cancer [15]. Although it was reported that dysregulation of lipid metabolism occurs in renal cell carcinoma [16] and SREBP1 was discovered to participate in the regulation of lipid metabolism [17], the mechanism underlying these aberrations in lipid homeostasis in RCC is not well understood and needs further analysis.

In this research, we revealed that SETD8 was overexpressed in RCC tissues and cells and had prognostic value for overall survival in RCC patients. SETD8 promoted cell growth and metastasis by regulating lipid metabolism via epigenetic transcriptional activation of SREBP1 in ccRCC cells. SETD8 downregulation impeded malignant tumor progression in a mouse xenograft model. In addition, we also found that ubiquitin-specific peptidase 17 (USP17) stopped SETD8 from post-translational degradation via deubiquitination to induce SETD8 overexpression and facilitate its oncogenesis in ccRCC. Altogether, the USP17/SETD8/SREBP1 pathway plays a pivotal role in modulating lipid metabolism and enhancing cell proliferation and metastasis in ccRCC. Thus, this pathway might be a novel therapeutic target and SETD8 could become a promising prognostic biomarker for treating RCC.

2. Materials and methods

2.1. Ethics statement

RCC specimen collection was approved based on the signed informed consent from each patient. Implementation of the research was supported by the Institutional review board of Qilu Hospital of Shandong University. Ethical approval for research relating to animals was received from the Institutional Animal Care and Use Committee of Qilu hospital.

2.2. Patients and clinical specimens

Both tumor and adjacent normal tissue specimens were collected from 121 patients with ccRCC by radical nephrectomy at the department of urology of Qilu hospital of Shandong University between 2006 and 2015. All specimens were clinically and pathologically confirmed and classified according to the 2017 TNM staging manual of AJCC [17]. The pathological grade was determined using the Fuhrman nuclear grading system [18].

2.3. Cell culture and reagents

786O and A498 clear cell renal cell lines and Human Embryonic Kidney (HEK) 293T cells were purchased from Cell Bank of Chinese Academy of Sciences (Shanghai, China). 786O and A498 cell lines were cultured in RPMI 1640 medium (Gibco). 293T cells were cultured in high-glucose DMEM medium (Gibco). All media were supplemented with 10% FBS (Gibco), 100 U/ml penicillin, 100 μg/ml streptomycin and 12.5 U/ml nystatin (Solarbio). All cells were cultured at 37 °C in an incubator with constant 5% CO^2. UNC0379 was purchased from TargetMol (T1841). Palmitic acid was purchased from sigma (PHR1120).

2.4. Bioinformatics analysis

UALCAN (http://ualcan.path.uab.edu/index.html) was used to analyze the gene expression and correlations between 522 ccRCC and 72 normal kidney specimens from The Cancer Genome Atlas (TCGA) database (http://cancergenome.nih.gov). The Gene Set Enrichment Analysis (GSEA) tool (https://www.broadinstitute.org/gsea/) was adopted to determine certain pathways in which SETD8 played a statistically significant role on the basis of RNA-seq data from the GEO database (GSE81626) (https://www.ncbi.nlm.nih.gov/geo/). Spearman's correlation analysis was conducted in the light of TCGA database through GEPIA online website (http://gepia.cancer-pku.cn/index.html).

2.5. siRNA transfection

siRNA duplexes of SETD8 (si-SETD8_1/2), SREBP1 (si-SREBP1_1/2) and USP17 (si-USP17_1/2) were synthesized by GeneChem. Transfection of 786O and A498 cells were conducted using Lipofectamine 2000 reagent (Invitrogen) according to its manufacturer's protocol. All siRNA sequences are provided in Supplementary Table S1.

2.6. Plasmid and recombinant lentivirus constructs

To construct the SETD8-shRNA lentivirus, an effective siRNA sequence of SETD8 was incorporated into the lentiviral vector pLent-U6-GFP-Puro (Vigene Biosciences, Inc). The shRNA sequence was as follows: GGGCTGCTACATGTACTATTTCAAGAGAATAGTACATGTAGCA GCCCTTTTTT. After extracting and purifying plasmids of SETD8-shRNA or control-shRNA, pLent-U6-GFP-SETD8-shRNA or control-shRNA was respectively cotransfected with two packaging plasmids, PMD1G and psPAX2, into 293T cells using jetPRIME (Polyplus-transfection, Illkirch, France). At 48 h, supernatants containing SETD8-shRNA lentivirus were collected to infect 786O cells 3–5 times. Then, infected 786O cells were selected by applying puromycin (4 μg/ml) to become stable cell lines for further experiments. SETD8 expression was determined by RT-qPCR and Western blot.

2.7. RNA isolation, reverse transcription and RT-qPCR

Total RNA was extracted from tissue samples or cultured cells using RNAfast2000 kit (Fastagen). cDNA was synthesized from a total of 1 μg RNA by using the PrimeScript™ RT reagent Kit (TAKARA). Real-time quantitative PCR was performed using SYBR Green of RT Master Mix (TAKARA). Relative mRNA expression of the target gene was normalized to the expression of the endogenous control GAPDH with the comparative C (T) (2(−ΔΔCT)) method. The list of primer sequences' information is displayed in Supplementary Table S2.

2.8. Immunoblotting and immunoprecipitation (IP) assay

Tissue specimens and cultured cells for total protein extraction were lysed using RIPA lysis buffer supplemented with 1% PMSF (Beyotime). The protein concentration was determined using a BCA Protein Assay Kit

(Beyotime). Then, 30 μg of total protein was used for Western blot analysis through SDS–PAGE according to the standard procedure [19]. First, protein was separated by 10% SDS-polyacrylamide gels and transferred onto PVDF membranes. Afterward, the membrane was blocked with 5% skimmed milk for 1 h and incubated with a specific primary antibody at 4 °C overnight. The next day, the membrane with protein was washed 30 min in TBST and incubated with a secondary antibody for 1 h at room temperature. Finally, protein images were obtained through enhanced chemiluminescence (ECL). The cells were lysed with IP lysis buffer supplemented with protease and phosphatase inhibitor cocktail (New Cell & Molecular Biotech Co. Ltd). Cell lysates were first incubated with agarose protein A + G (Santa Cruz Biotechnology, Dallas, Texas, USA) and then anti-His (Abcam, USA) or anti-Flag (Proteintech Group, Inc., USA) at 4 °C overnight. The purified protein supernatants were added to IP loading buffer and then used to detect protein expression. Immunoblotting was conducted according to a previously described procedure. Detailed information on all antibodies is provided in Supplementary Table S3.

2.9. Immunohistochemistry

A set of tissue chips/microarrays, renal cancer specimens and xenograft tumors were used to conduct immunohistochemistry (IHC) analyses in accordance with the instructions of the Two-step IHC Kit (ZSGB-BIO). For IHC quantification, the staining area score was classified as 0 (0% stained), 1 (1–25% stained), (26–50% stained), and 3 (51–100% stained); the staining intensity was classified as 0 (negative), 1 (low), 2 (moderate) and 3 (high). The final score was calculated using the following formula: final score = staining area score × staining intensity score. The classification of the final score was as follows: a score greater than 6 represented strong staining; 4–6 represented moderate staining; 2–3 represented weak staining; and less than 2 represented negative staining. Information on the primary antibodies is shown in Supplementary Table S3.

2.10. Oil Red O staining

Renal cells were seeded into 6-well plates, transfected with certain siRNAs or treated with an inhibitor for 48 h. After the supernatants were discarded, all cells were rinsed three times with PBS, fixed with 4% paraformaldehyde for 30 min, washed three times with PBS, stained with Oil Red O (ORO) solution for 1–4 h, washed with PBS, destained with isopropanol for 5 s, rinsed again three times with PBS, and stained with Mayer's hematoxylin for 2 min. After this, they were washed three times with distilled water and differentiated by 1% acid alcohol. For quantification, we counted cell numbers by randomly selecting five 100/200 × fields under a microscope. OCT-embedded fresh tissue specimens were first sectioned into 8 μm slices and then stained according to a previous protocol.

2.11. Chromatin immunoprecipitation

Chromatin immunoprecipitation (ChIP) assays for 786O and A498 ccRCC cells were performed according to the manufacturer's protocol of the ChIP Assay Kit (Cell Signaling Technology). Cells were treated with 1% formaldehyde for the crosslinking of protein with DNA and then sonicated to obtain DNA fragments with lengths of 500–800 base pairs. Solutions containing DNA fragments were incubated with *anti*-SETD8 (Cell Signaling Technology, MA), *anti*-H4K20me1 antibody (Abcam, USA), or IgG negative control at 4 °C overnight on a rotator. Immunocomplexes were purified and used to perform reverse transcription real-time quantitative PCR for the detection of certain DNA fragments. GAPDH was used as a negative control. The list of primer sequence information is displayed in Supplementary Table S2.

2.12. Colony formation assay

786O or A498 cells (500 per well), stably transfected with SETD8-shRNA, SREBF1-shRNA or control shRNA, were seeded into 6-well plates and then cultured for 2 weeks. Afterward, cell colonies were fixed by 4% paraformaldehyde for 20 min and stained with 0.1% crystal violet for 10 min.

2.13. Wound-healing assay

Cells were seeded into 6 cm culture dishes and transfected with SETD8/SREBF1 siRNAs for 24 h. Then, the cells were reseeded into 6-well plates and scratched with a sterile 200-μl pipette tip. Images of wounds were captured at 0 and 24 h.

2.14. Cell migration and invasion assay

The migration and invasion assays were performed as follows. A total of 1×10^4 786O or A498 cells previously transfected with SETD8/SREBF1 siRNAs or SREBF1 vector for 24 h were seeded into upper Transwell chambers (Corning Costar, Lowell, USA) containing 8-μm polycarbonate membrane filters, while 800 μl serum-free medium containing 15% FBS was supplemented in the bottom chambers. Cells were cultured for another 24 h and then stained with 0.1% crystal violet. Images were captured under a microscope, and cell numbers were counted in five random fields. Notably, diluted Matrigel (ratio: 1:8) (Corning Costar, USA) was added for the invasion assay.

2.15. Cycloheximide (CHX) half-life assay

RNAi transient transfection was performed for RCC cells. After treatment with 50 μg/ml cycloheximide (CHX), the cells were collected over certain periods of 0, 0.5, 1 and 2 h. Protein expression of USP17 was analyzed by immunoblotting. Information on the primary antibodies is shown in Supplementary Table S3.

2.16. Subcutaneous xenograft tumorigenesis

A total of 1×10^7 786O cells stably transfected with SETD8-shRNA or control-shRNA were suspended in a 0.15 ml mixture of PBS/Matrigel (ratio: 1/3) and injected into the subcutaneous skin of BALB/c nude mice (4 weeks old, female). The tumor growth and weight of mice were monitored and recorded periodically. The volume of xenograft tumors was calculated using the following formula: volume (mm^3) = length (mm) × width^2 (mm)/2. The observation of the survival state of all mice continued for four months. The surviving mice were all sacrificed humanely. Tumors were collected and fixed with 10% neutral formalin fix solution and then used to perform IHC.

2.17. CCK-8 assay

A Cell Counting Kit (CCK-8) assay was performed according to the manufacturer's instructions (Dojindo Molecular Technologies, Shanghai, China), to evaluate the proliferation of renal cancer cells. In general, 3×10^3 renal cells per well suspended in 100 μl of complete medium were seeded into 96-well plates and cultured in an incubator with 5% CO^2 at a constant 37 °C. Renal cells were then transfected with relevant shRNAs or plasmids of SETD8 or SREBP1 or processed with the SETD8 inhibitor UNC0379 after being cultured for 24 h. Forty-eight hours later, the cell medium per well was replaced by fresh medium with 10 μl CCK-8 reagent. After incubating for 1 h at 37 °C, the OD value

of each well was determined by an enzyme-linked immunosorbent assay microplate reader (Tecan Trading AG, Switzerland) at 450 nm.

2.18. Statistical analysis

Basically, data were displayed as the mean ± SD in all figures. SPSS 20.0 (IBM) and PRISM 8.4 (GraphPad Software) were adopted to conduct the statistical analysis. Data from two groups were statistically determined by Student's *t-test*, while multiple comparisons were determined by one-way ANOVA. Pearson's coefficient was employed to assess the correlation between two genes. Categorical data were evaluated by Pearson's chi-square test. Hypothesis tests were all two-sided. A P value < 0.05 was regarded as statistically significant.

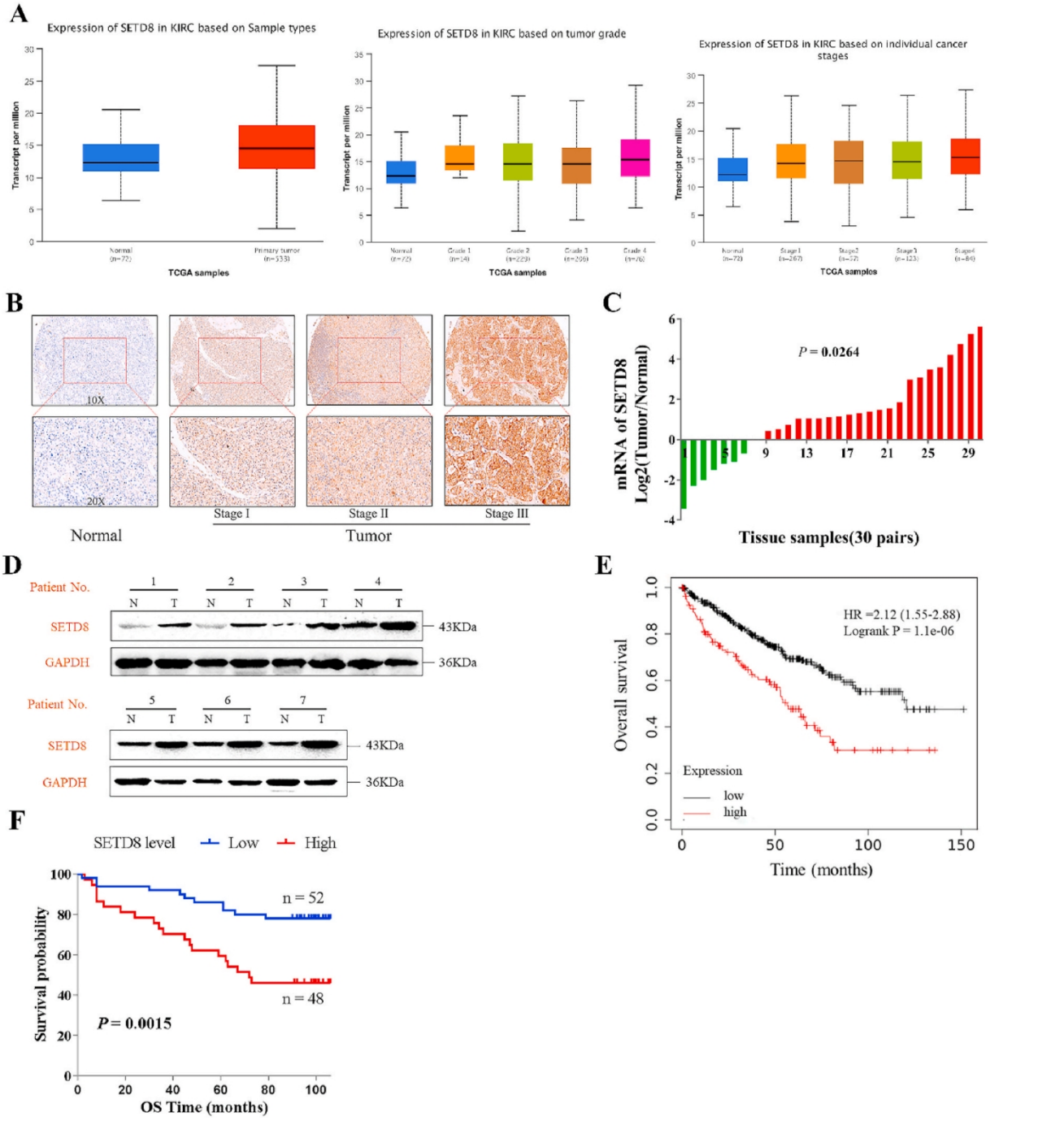

Fig. 1. Elevated SETD8 expression in RCC tumors and its correlation with clinical characteristics and outcomes. (A) Box plots of increased relative median expression of SETD8 mRNA in tumor and adjacent normal samples or in samples with different grades and stages from TCGA ccRCC database ($P < 0.01$). (B) Representative images of the expression of SETD8 protein in ccRCC tumor tissues with different stages and corresponding normal tissues by IHC staining analysis (scar bars: 100 μm in 100x and 50 μm in 200x). (C) The relative mRNA expression of SETD8 by qPCR analysis in ccRCC tumor tissues and paired normal tissues (n = 30 pairs). (D) The protein expression of SETD8 in 7 pairs of ccRCC tumor tissues and matched noncancerous tissues (n = 7 pairs). Kaplan–Meier plots of overall survival in ccRCC patients based on the SETD8 expression levels in cancerous tissues from TCGA database (E) or obtained from surgery in Qilu hospital (F). Log-rank test was used to determine statistical significance by comparing two groups with indicated numbers.

3. Results

3.1. SETD8 is overexpressed and prognostic for poor survival outcome in ccRCC tumors

SETD8 mRNA expression in renal cancerous and normal tissues was determined by an analysis of the TCGA dataset through the UALCAN online website (http://ualcan.path.uab.edu/analysis.html). The results demonstrated that SETD8 mRNA expression was higher in tumor tissues than in normal tissues and positively correlated with tumor grades and stages (Fig. 1A). Additionally, the SETD8 protein expression level was also proven to be elevated in renal tumors compared with matched

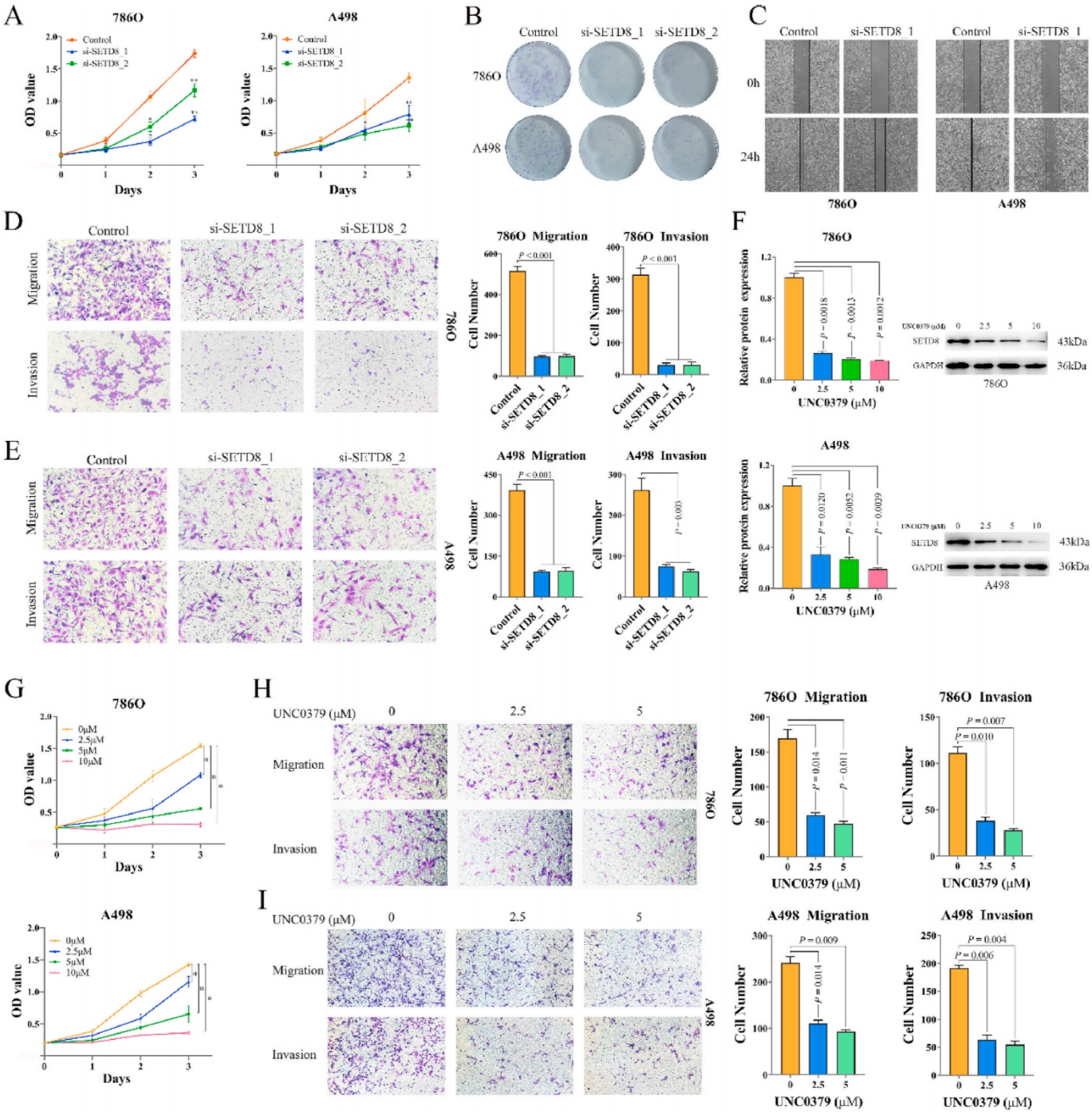

Fig. 2. Genetic and chemical SETD8 inhibitions attenuate cell proliferation and metastasis of ccRCC cells in vitro. (A) CCK-8 assays indicated that depletion of SETD8 by siRNA impeded cell proliferation in 786O (left) and A498 (right). Three independent experiments were performed in triplicate. (B) Colony-formation assays suggested that SETD8 downregulation decreased the abilities of colony formation (n = 3). (C) Wound healing assays demonstrated cell movement decreased after SETD8 inhibition (n = 3). (scar bars: 100 μm in 100x) (D, E) Transwell assays showed that SETD8 inhibition significantly blocked the abilities of cell migration and invasion (n = 3). (scar bars: 100 μm in 100x) (F) The Western blot analysis (right) and corresponding quantification of Western blot (left) were conducted to verify the effect of SETD8 inhibition by its specific inhibitor UNC0379 with different concentrations (0, 2.5, 5 and 10 μM). (G) CCK-8 assays indicated that cell growth was blocked more dramatically with the increasing concentrations of UNC0379. Three independent experiments were performed in triplicate. (H) and (I) Transwell assays displayed that chemical depletion of SETD8 abated the capacities of cell migration and invasion in ccRCC cell lines (n = 3). (scar bars: 100 μm in 100x).

normal tissues through an IHC assay of the tissue microarray (TMA) (Fig. 1B). In addition, thirty pairs of renal cancerous and matched paired normal tissues collected from clinical patients who underwent surgery were also used to perform qPCR assays and western blotting to determine the SETD8 mRNA (Fig. 1C) and protein levels (Fig. 1D), respectively. Similar to the previous result, SETD8 expression was upregulated in the majority of renal tissues (22/30) compared with paired normal tissues ($p = 0.0264$). Furthermore, a Kaplan–Meier analysis was performed using the Kaplan–Meier Plotter online website (http://kmplot.com/analysis/index.php?p=background) based on the TCGA dataset to evaluate the correlation between SETD8 expression and the survival outcome of the TCGA cohort of ccRCC patients (Fig. 1E). The mean expression level was defined as a cutoff, and all patients were separated into two groups with high or low SETD8 expression. Moreover, Kaplan–Meier analysis using GraphPad Prism software was also used to determine the correlation between SETD8 expression and the overall survival of clinical ccRCC patients (Fig. 1F). All patients were divided into two cohorts with high or low SETD8 expression based on the expression level of SETD8 assessed by IHC (H-score = 4) as a cutoff. These data showed that patients with lower SETD8 expression had longer overall survival. Taken together, SETD8 plays a pivotal significance in RCC development and may be a prognostic biomarker for RCC detection.

3.2. SETD8 inhibition by siRNAs or inhibitor UNC0379 attenuates the biological phenotype of renal cells in vitro

To determine the mechanism by which high SETD8 expression affects ccRCC initiation and development, we investigated the effects of SETD8 inhibition on the biological functions of ccRCC cell lines. First, we examined the proliferative ability of 786O and A498 cells, which were observed to be significantly restrained after SETD8 depletion, through a Cell Counting Kit-8 (CCK-8) detection assay (Fig. 2A). In addition, by conducting a colony formation assay, we determined that the colony-forming capacity was also significantly abated for ccRCC cells with stable depletion of SETD8 in comparison with intact cells (Fig. 2B). Moreover, a wound healing assay indicated that knockdown of SETD8 expression significantly blocked cell movement (Fig. 2C). A similar phenomenon was observed based on the Transwell assay (Fig. 2D–E). The cell migration and invasion rates were both apparently diminished as SETD8 expression was depleted.

To further confirm these findings, we adopted the small molecule SETD8 inhibitor UNC0379 to achieve pharmacological inhibition instead of genetic inhibition. UNC0379 is a selective, substrate competitive inhibitor of the *N*-lysine methyltransferase SETD8 and has high selectivity over 15 other methyltransferases, including G9a, SETDB1, and SETD7 [19]. Western blot assays were performed to determine the effective concentrations of UNC0379 on SETD8 expression inhibition at the protein level (Fig. 2F). UNC0379 treatment for pharmacological inhibition of SETD8 also led to significant suppression of RCC cell proliferation by performing a Cell Counting Kit-8 (CCK-8) detection assay (Fig. 2G). As expected, Transwell assays showed that RCC cell migrative and invasive capabilities were significantly suppressed after UNC0379 treatment (Fig. 2H–I). In summary, these results strongly indicate that SETD8 plays a crucial role in regulating RCC cell growth and metastasis.

3.3. Genetic depletion of SETD8 significantly impedes tumor growth in xenograft implantation models of ccRCC cells

To evaluate the impacts of SETD8 genetic inhibition on tumor growth in vivo, we then generated stable shRNA targeting SETD8 based on an effective siRNA sequence and established stably expressing SETD8-shRNA cells in ccRCC 786O cell lines. SETD8-shRNA or control-shRNA cells were implanted into the subcutaneous flank of BALB/c nude mice. Tumor growth was monitored and recorded periodically. Xenograft tumor initiation of SETD8-shRNA cells was significantly prolonged compared to that of control-shRNA cells, and the tumor growth rate was much slower in the SETD8-shRNA group than in the control group (Fig. 3A, B and 3D), while mouse body weights showed almost no changes (Fig. 3C). In conclusion, these data demonstrate that depletion targeting SETD8 expression in ccRCC cells significantly restrained tumor xenograft growth.

3.4. SETD8-mediated H4K20me1 directly activates SREBP1 expression at the transcriptional level

To further reveal the in-depth mechanism contributing to the SETD8 regulation of cell proliferation and metastasis in RCC cells, we conducted a bioinformatics analysis on the basis of RNA-seq transcriptome data. Preliminary studies were performed to establish the conditions for effective depletion of SETD8 and minimize the effects on cell viability; then, siCTR and siSETD8 groups were used to conduct RNA-seq transcriptome analyses [20]. All features in the dataset are depicted as a clustered heatmap (Supplementary Fig. S1 and Table S5). GSEA (gene set enrichment analysis) showed enrichment in the fatty acid metabolism pathway (Fig. 4A). SETD8 (also named KMT5A) participated in this pathway and ranked first with the most significant rank metric score (3.572), indicating that SETD8 might play an essential role in contributing to the regulation of fatty acid metabolism (Supplementary Table S6). Various kinds of key enzymes are involved in the process of lipid metabolism, including ACACA, FASN and SCD1, as illustrated in Fig. 4B. Then, we evaluated whether there was any relationship between SETD8 and these enzymes by performing Western blotting. Surprisingly, SETD8 silencing resulted in obvious downregulation of ACACA, FASN and SCD1 protein expression (Fig. 4C). As previously described, sterol regulatory element binding protein 1 (SREBP1) is the pivotal transcription factor that contributes to lipid metabolism by regulating the expression of key enzymes, including ACACA, FASN and SCD1 [21–23]. In view of these findings, we proposed that SETD8 might modulate all these enzymes by governing SREBP1 expression.

With this hypothesis, we then investigated the relationship between SETD8 and SREBF1 mRNA expression. As presented in Fig. 4D, we discovered that SETD8 transcript abundance had a positive correlation with that of SREBF1 by conducting Spearman's correlation analysis with TCGA cohort of RCC tumors ($R = 0.29$, $P = 6.2e^{-13}$). Furthermore, we found that SETD8 genetic silencing could lead to downregulation of SREBP1 expression at both the mRNA and protein levels (Fig. 4E–F) and vice versa, namely, significant elevation of SREBP1 expression with SETD8 overexpression (Fig. 4G–H). SETD8 is the only histone methyltransferase that can monomethylate histone 4 lysine 20, and its epigenetic modification is involved in DNA replication, cell cycle regulation, chromatin transcription, and so on. To elucidate the molecular mechanism of SETD8-mediated regulation of SREBP1 expression, a ChIP assay was adopted to evaluate whether there was any alteration in the promoter region of SREBF1 when SETD8 expression was silenced. Several primer pairs were designed for amplifying different regions on the SREBF1 gene locus (Fig. 4I). SETD8 expression was depleted in both 786O and A498 cells and led to decreased expression of H4K20me1 (Fig. 4F). The results of the ChIP assay demonstrated that SETD8 had a significant occupancy in the SREBF1 gene locus (Fig. 4J), and the regional occupancy of the H4K20me1 mark was also abolished after SETD8 silencing (Fig. 4K). In summary, all observations implied that SETD8 mediated H4K20me1 and then altered the chromatin pattern on the promoter region of SREBF1 to directly activate genetic transcription.

3.5. SETD8 promotes cell proliferation, metastasis and lipogenesis of RCC via SREBP1

As verified above, SETD8 induced advanced transcriptional expression of SREBP1 as a direct target by epigenetic chromatin remodeling. We then sought to confirm whether SETD8 exerted its protumor activity

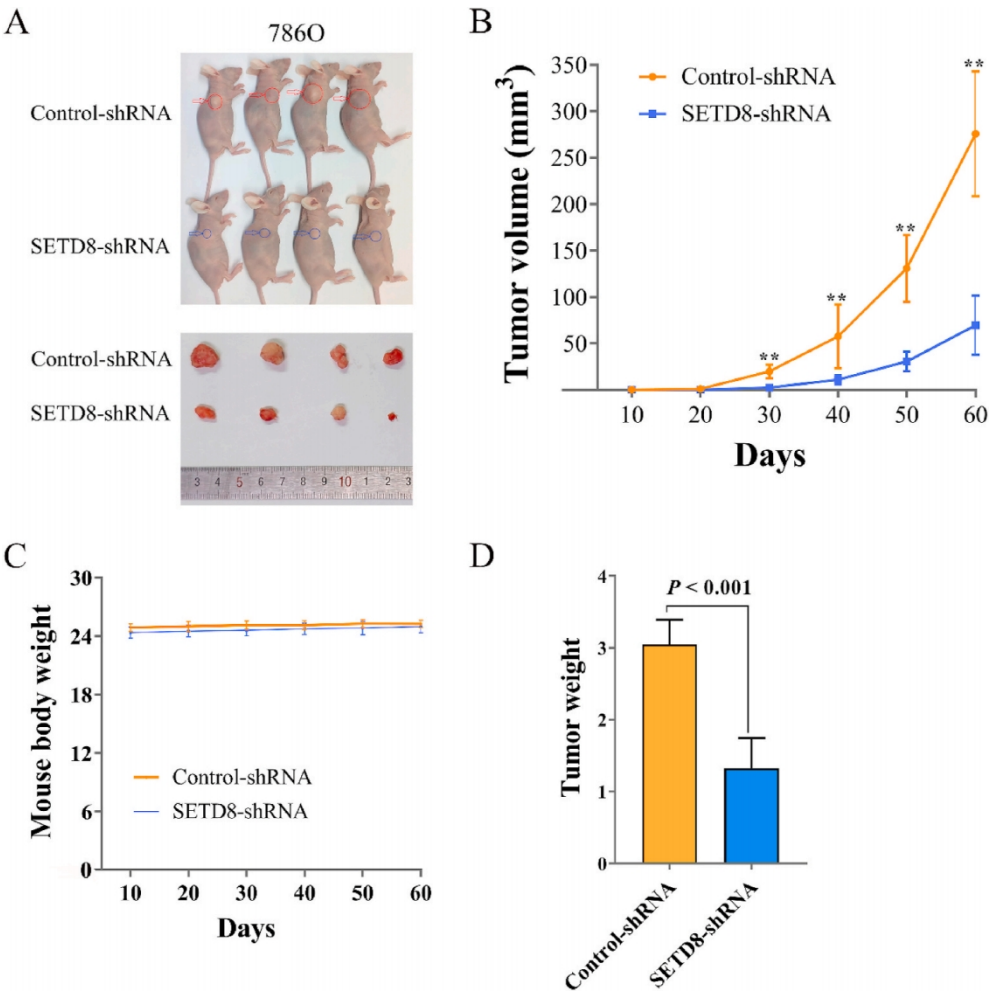

Fig. 3. SETD8 silencing impairs tumorigenic potential and shortens survival probability of ccRCC in vivo. (A) 786O ccRCC cells were stably transfected with SETD8-shRNA or Control-shRNA and then injected subcutaneously into BALB/c nude mice (n = 4). Tumor sizes, weights and mice body weight were measured periodically. Upper panel: the display of representative images of nude mice. Lower panel: images of tumors corresponding to cells-injected nude mice in the upper panel. (B) The dynamic growth curves of tumor volume indicate distinct increasing rates of tumors in two groups during 8 weeks. (C) Mouse body weights were measured periodically to observe the effects of tumor burden. (D) Tumor weight of nude mice implanted with the stable SETD8 silencing or control-shRNA cells was measured at the end of collection of tumors. $^{**}P < 0.01$.

through SREBP1 by performing biological functional assays. First, CCK-8 assay and colony formation assay were performed to determine the effects of SETD8 depletion and SREBP1 overexpression on cell proliferation. These results indicated that the proliferation of 786O and A498 cells with SETD8 silencing was significantly abated, while this abatement was abolished when SREBP1 expression was promoted by transfection of the SREBP1 vector into RCC cells (Fig. 5A–B). Second, a similar trend was also observed in the detection of migratory (Fig. 5C–D) and invasive (Fig. 5E–F) abilities. Transwell assays demonstrated that these functions were decreased when SETD8 was knocked down and reversed with SREBP1 overexpression. Finally, by adopting an ORO staining assay, we discovered that genetic knockdown of SETD8 impeded lipogenesis of 786O and A498 cells, which almost returned to the previous level, followed by transfection of the SREBP1 vector into RCC cells (Fig. 5G). Western blots were performed to confirm whether there were corresponding alterations in the expression of key enzymes associated with the lipid metabolism pathway. As shown in Fig. 5H, the results indicated that SETD8 significantly regulated the protein expression of ACACA, FASN and SCD1 via SREBP1. Taken together, these data implied that SETD8 affected RCC cell biological functions by modulating the gene expression of SREBP1.

Next, we investigated whether SETD8 or SREBF1 transcript abundance were significantly correlated with key enzymes, including ACACA, FASN and SCD1, in human renal tumor tissues from the TCGA database. As depicted in Fig. 6A–B, the specific results were displayed as follows: SETD8 had a positive correlation with three key enzymes (ACACA: R = 0.53, $P = 5.2e^{-46}$; FASN: R = 0.35, $P = 2e^{-19}$; SCD1: R = 0.2, $P = 5.7e^{-7}$), as did SREBF1 (ACACA: R = 0.17, $P = 1.2e^{-5}$; FASN: R = 0.38, $P = 1.8e^{-22}$; SCD1: R = 0.46, $P = 2.1e^{-33}$). In addition, we conducted IHC assays with xenograft tumors to further validate the expression patterns of these key enzymes in SETD8-depleted cells. As anticipated, the expression of these enzymes and SREBP1 significantly declined as SETD8 was knocked down. Finally, we also examined the expression of KI67 by IHC, and it was significantly decreased in the SETD8-shRNA tumors compared to that in the control-shRNA tumors, implying that the proliferation of ccRCC cells was impaired in vivo.

3.6. Ubiquitin-specific peptidase 17 (USP17) posttranslationally stabilizes SETD8 through deubiquitination

After determining that SETD8 facilitated the proliferation and metastasis of RCC cells by regulating SREBP1-mediated lipid metabolism, we sought to discover the method by which SETD8 maintained high expression in RCC cells. Recently, it was reported that ubiquitin-specific peptidase 17–like family member (USP17), one of the deubiquitinases (DUBs), stabilized SETD8 during the posttranslational process and then contributed to its prevention of cellular senescence in breast cancer cells [24]. Surprisingly, studies concerning USP17 were scarce for RCC. Thus, we sought to determine whether USP17 could affect the SETD8 expression level in RCC cells.

Initially, we genetically knocked down the expression of USP17 in 786O and A498 cells by RNAi. Thereafter, the expression of SETD8 was examined at both the mRNA and protein levels using qPCR and Western blot, respectively. As expected, the mRNA expression of SETD8 did not fluctuate significantly when USP17 was knocked down (Fig. 7A), while the protein expression was significantly decreased (Fig. 7B). We next

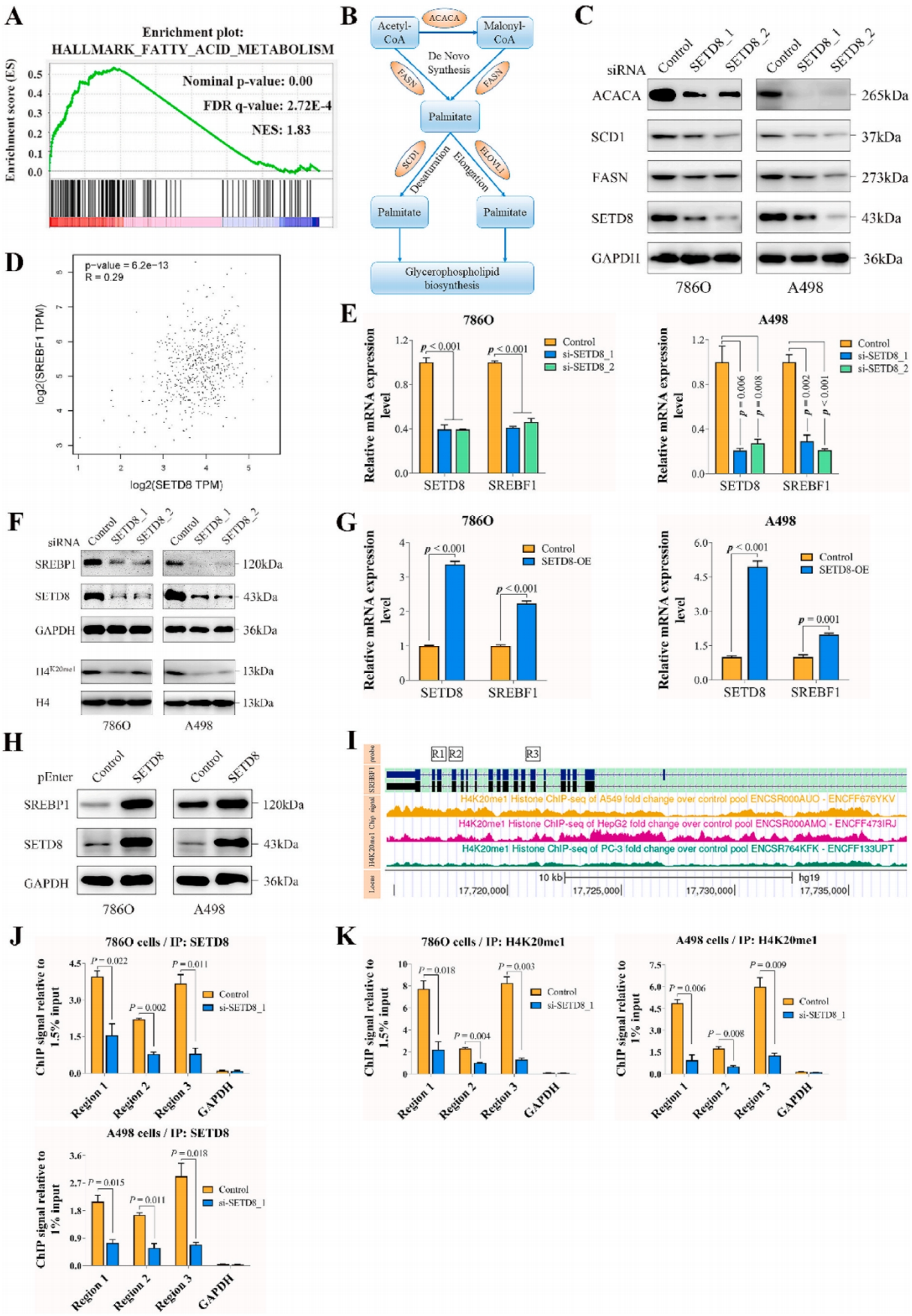

(caption on next page)

Fig. 4. SETD8 epigenetically enhances the transcriptional expression of SREBF1 as a direct target. (A) GSEA (Gene Set Enrichment Analysis) of the fatty acid metabolism pathway (nominal p value = 0.00, FDR q-value = 2.72e-4, NES = 1.83) after SETD8 silencing. (B) Systematic flowchart of fatty acid synthesis pathway and the key enzymes in this pathway. (C) Western blot was conducted to evaluate the relationship between SETD8 and three key enzymes in the fatty acid metabolism pathway after SETD8 was knocked down in 786O and A498 cells (n = 3). GAPDH was as loading control for densitometric analysis of protein levels. (D) Positive correlation of SETD8 and SREBF1 mRNA transcript abundance in TCGA ccRCC database. The relationship between SETD8 and SREBP1 was assessed by qPCR (E) and Western blot (F) after SETD8 was silenced in 786O and A498 cells (n = 3). The relationship between SETD8 and SREBP1 was assessed by qPCR (G) and Western blot (H) after SETD8 was overexpressed in 786O and A498 cells (n = 3). (I) Display of the SREBF1 gene structure and its genome location. Relative positions of the primers as R1, R2, and R3 for the ChIP assay are shown in the Probe track. Relative positional occupancy of the H4K20me1 mark annotated in the ENCODE data in the indicated cell lines is adapted at the UCSC genome browser. (J, K) Chromatin immunoprecipitation (ChIP) analysis was performed for evaluation of chromatin association of SETD8 and the H4K20me1 mark within the SREBF1 promoter region. IgG, SETD8 or H4K20me-1 antibodies were used to precipitate DNA fragments in 786O and A498 cells transfected with control or SETD8 siRNAs. The relative expressions of DNA fragments were quantitatively analyzed by qPCR, and normalized to the values of IgG. GAPDH gene serves as appropriate control.

performed a cycloheximide half-life assay to observe SETD8 protein alterations in different periods. This result indicated that degradation of the SETD8 protein was quicker when USP17 was depleted by RNAi. In other words, the SETD8 protein was much more stable in the presence of USP17 (Fig. 7C and D). Additionally, we further verified that there was a protein interaction between USP17 and SETD8 by conducting immunoprecipitation. Endogenous USP17 was detected by incubation with an *anti*-SETD8 primary antibody, thus demonstrating that USP17 bound to SETD8 and stabilized its protein structure by deubiquitination, as described previously [24] (Fig. 7E). Furthermore, we investigated the effect of USP17 depletion on the expression of SREBP1 and key enzymes in lipid metabolism. As anticipated, the expression of SREBP1, ACACA, FASN and SCD1 was significantly decreased by USP17 depletion-mediated SETD8 degradation (Fig. 7F). Conversely, overexpression of USP17 led to an increase in the expression of SETD8, SREBP1 and key enzymes (ACACA, FASN and SCD1) in the fatty acid metabolism pathway, as detected by immunoblotting analysis (Fig. 7G). In renal cancer cells, USP17-induced SETD8 overexpression by deubiquitination boosted lipogenesis by epigenetically modulating SREBP1-mediated lipid metabolism and further promoted cell proliferation and metastasis of ccRCC (Fig. 8).

4. Discussion

Epigenetic regulation of DNA-templated processes has a become a popular research topic over the last decades due to its closer correlation with cancer [25]. Generally, it includes DNA methylation [26], nucleosome remodeling [27], ncRNA-mediated targeting regulation [28] and histone modification [29], which are all extremely fundamental for the genesis of cancers. In particular, histone modifications, which are classified into histone acetylation, methylation, phosphorylation or related gene mutation, have aroused widespread attention because of their roles in contributing to the progression of cancer [4]. Methyltransferases (KMTs) are mainly responsible for the regulation of lysine residues within histones [30].

SETD8 is one of the KMTs that was first purified and found as a histone methyltransferase by Fang Jia and his colleagues [31]. Previous findings revealed that there were multivalent interactions between SETD8 and nucleosome substrates when the enzyme bound and methylated them [32]. Furthermore, SETD8 is involved in several biological processes, such as cell cycle progression [33], transcription repression [34] and activation [35], DNA damage response [36] and adipogenesis [9]. Moreover, increasing evidence has revealed that SETD8 plays a significant role in the progression of various kinds of cancers, including neuroblastoma [20], glioma [37], gastric adenocarcinoma [38], pancreatic cancer [39], and breast cancer [40]. However, studies corresponding to the significance of SETD8 in renal cancer are scarce. In this research, we thoroughly elucidated that the expression of SETD8 was significantly elevated in human RCC tissues and cells and showed that its high expression was positively correlated with tumor grade and stage and predictive of the overall survival of RCC patients. Based on the observation of its effects on the growth of the mouse xenograft model, we further confirmed that SETD8 depletion blocked the progression of renal tumors in vivo. Moreover, SETD8 downregulation by siRNA and the inhibitor UNC0379 abated the proliferation and metastasis of RCC cells in vitro.

Characteristic changes in many features of cancer cells contribute to their powerful survival advantage in terms of growth and metastasis. Notably, it is universally acknowledged that metabolic pathways reprogram dramatically in malignant tumors and are considered a hallmark of cancer [41]. The most remarkable feature in metabolic reprogramming for ccRCC is lipid deposition. A prominent alteration in lipid metabolism inversely exerts a considerable influence on the regulation of many cellular processes, such as cell growth, proliferation, differentiation, survival, motility, and membrane homeostasis [42].

The key transcription factors for the regulation of lipid metabolism under both physiological and pathological conditions are sterol regulatory element-binding proteins (SREBPs), which can control the expression of genes involved in lipid synthesis and uptake [43]. SREBPs are a family of transcription factors consisting of three members with basic-helix-loop-helix leucine zipper structures, such as SREBP1a, SREBP1c and SREBP2 [44]. SREBP1a and SREBP1c are encoded by the gene SREBF1 and thus are similar in structure, and they can both regulate de novo synthesis of fatty acids and cholesterol as well as cholesterol uptake; however, SREBP2 is encoded by the gene SREBF2, and it is mainly responsible for the regulation of cholesterol synthesis and uptake [45–47]. Recently, SREBP1 was found to play a magnificent role in the progression of various cancers by impacting lipid metabolism [48,49]. In addition, SREBP1 was verified to modulate cell migration and invasiveness by several pathways [13,50–52].

Interestingly, SETD8 was demonstrated to participate in the regulation of distinct metabolic processes, such as mitochondrial metabolism [53], anabolic metabolism [40] and aerobic glycolysis [54]. Nevertheless, the relationship between the epigenetic modulator SETD8 and lipid metabolism and the underlying mechanism by which they affect proliferation and metastasis in ccRCC are rare and ambiguous. In this study, to explore the in-depth mechanisms underlying the promotion of the growth and metastasis of ccRCC cells, we first discovered that SETD8 participated in the regulation of lipid metabolism, namely, fatty acid synthesis, by bioinformatic analysis based on RNA-seq data from the GEO database (GSE81626). There are three key enzymes, ACACA, FASN and SCD1, in the process of fatty acid synthesis [55]. SETD8 silencing was detected to induce the downregulation of these three key enzymes together. SREBP1 regulates all of them as a key transcription factor in the regulation of fatty acid synthesis [45]. Surprisingly, a correlation analysis demonstrated that there was a positive correlation between the mRNA abundance of SETD8 and SREBP1. Finally, we comprehensively elucidated that SETD8 modulated the transcription of SREBP1 as a direct target by methylating the 20th lysine of histone 4 by ChIP assay and thus had enormous effects on the process of lipogenesis. In addition, we also proved that the SETD8 protein was posttranslationally stabilized by deubiquitination mediated by USP17, which is consistent with a previous study [24]. Ubiquitin-specific protease 17 (USP17) is an immediate early gene belonging to a subfamily of cytokine-inducible DUBs [56]. In addition, USP17, also named DUB3, is involved in the malignant transformation of cancer by deubiquitinating Cdc25 [57], which is

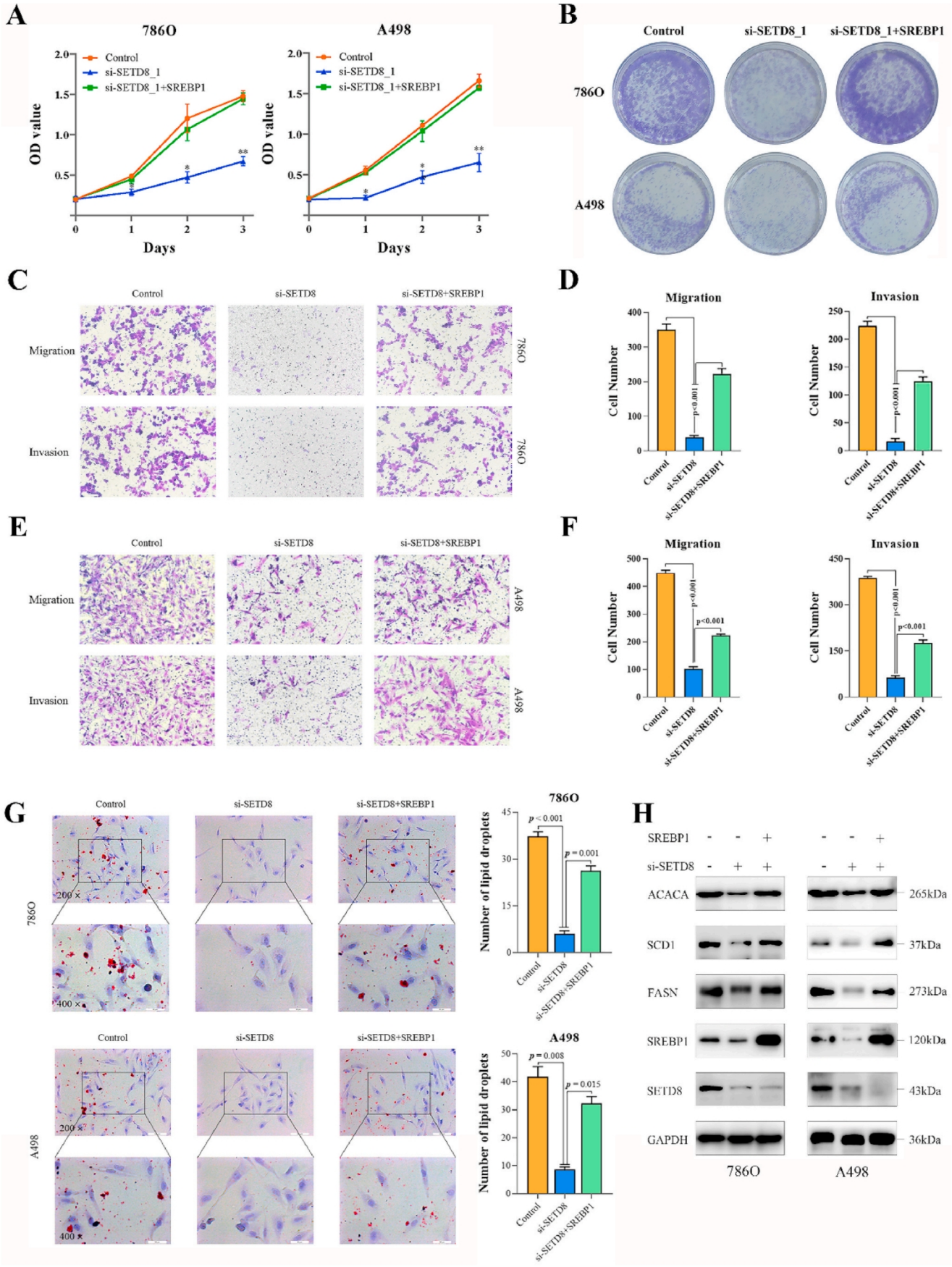

(caption on next page)

Fig. 5. SETD8 promotes lipogenesis, proliferation and metastasis of 786O and A498 ccRCC cell lines via upregulating SREBP1 expression. (A) CCK-8 assays demonstrated that SETD8 accelerated cell growth through SREBP1 in ccRCC cell lines (n = 3). (B) Colony-formation assays showed that SETD8 advanced the ability of colony formation by upregulating SREBP1 expression in 786O and A498 cells (n = 3). (*C*–F) Transwell assays revealed that depletion of SETD8 decreased the abilities of migration and invasion of 786O and A498 cells, while these phenomena were reversed after SREBP1 was overexpressed (n = 3). (scar bars: 100 μm in 100 ×) (G) ORO staining assays indicated that SETD8 reinforced de novo fatty acid synthesis of ccRCC cells through the upregulation of SREBP1 (n = 3). (scar bars: 100 μm in 100x and 50 μm in 200x) (H) Western blot analysis implied that SETD8 promoted biological functions of ccRCC cells by upregulating key enzymes as ACACA, FASN and SCD1 of lipid metabolism through SREBP1 in ccRCC cell lines. *$P < 0.05$; **$P < 0.01$.

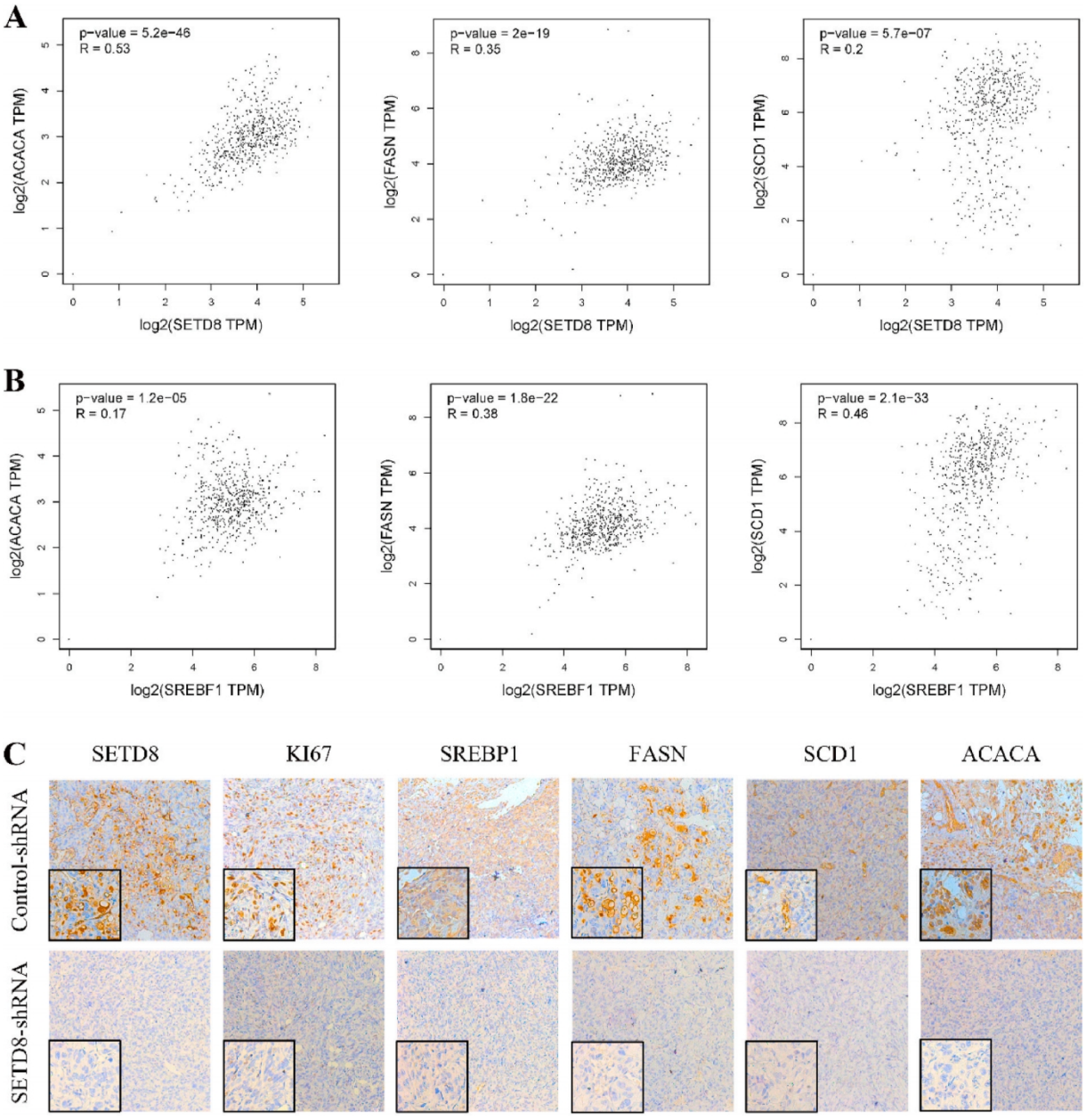

Fig. 6. SETD8 or SREBP1 mRNA and protein expressions are positively correlated with key enzymes of lipogenesis pathway in ccRCC tissues. (A) Positive correlation between the mRNA transcripts of SETD8 and three key enzymes as ACACA, FASN and SCD1 in TCGA dataset. (B) Positive correlation between the mRNA transcripts of SREBF1 and three key enzymes as ACACA, FASN and SCD1 in TCGA dataset. (C) The protein expressions of SETD8, SREBP1, ACACA, FASN and SCD1 in SETD8-shRNA and control-shRNA xenograft tumors were stained by immunohistochemistry. In addition, KI67 was also stained by IHC in SETD8-shRNA and control-shRNA xenograft tumors. Scar bars: 100 μm in 100x and 50 μm in 200x.

related to proliferation, and Snail [58,59] and Twist [60], which are closely linked to metastasis. Accumulating studies have demonstrated that USP17 is essential in the progression of different kinds of cancers [61–63]. However, the role of USP17 in renal cancer has not been previously reported. We first discovered that USP17 affected the lipid metabolism of RCC by stabilizing SETD8.

Limitations were observed in our present research. The whole study was conducted only using ccRCC as our subject due to the low number of nonccRCC patients. Thus, it is difficult to reach a confirmative conclusion on SETD8 expression in nonccRCC specimens and its underlying mechanism. With the rapidly widespread adoption of single-cell RNA sequencing (scRNA-seq), the puzzle might be solved soon. Moreover, in

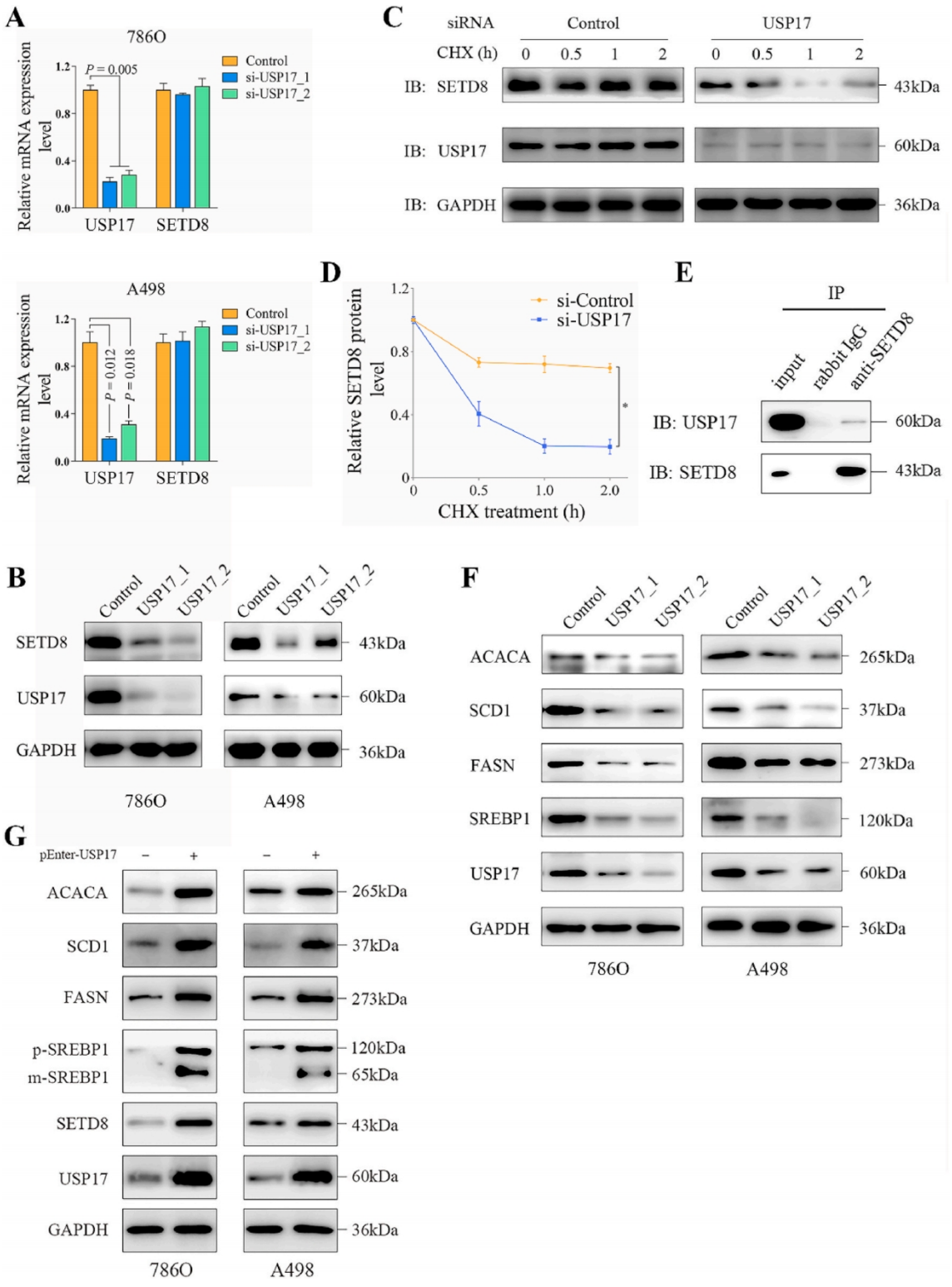

Fig. 7. The ubiquitin-specific protease 17 (USP17) post-translationally stabilizes SETD8 protein to facilitate the oncogenesis of SETD8 in ccRCC cells. (A) The quantitative qPCR analysis was conducted to evaluate the alteration of SETD8 mRNA expression in 786O and A498 cells (n = 3). (B) The Western blot analysis was performed to assess the change of SETD8 mRNA expression in 786O and A498 cells (n = 3). GAPDH was as loading control for densitometric analysis of protein levels. (C) 786O cells transiently transfected with the indicated siRNAs of USP17 were treated with CHX for a certain time point. The stability of SETD8 protein was evaluated at the indicated time point by Western blot analysis. (D) The curve of SETD8 protein alteration was significantly distinct between 786O cells with USP17 siRNAs and control. GAPDH was used as loading control for densitometric analysis of protein levels. (E) SETD8 antibody was used to immune-precipitate endogenous SETD8 protein from 786O cells, and endogenous USP17 bound with SETD8 was examined by immunoblotting. (F) USP17 depletion induced downregulation of SREBP1 and key enzymes (ACACA, FASN and SCD1) in the fatty acid metabolism pathway detected by immunoblotting analysis. (G) Overexpression of USP17 led to an increase in the expression of SETD8, SREBP1 and key enzymes (ACACA, FASN and SCD1) in the fatty acid metabolism pathway detected by immunoblotting analysis. GAPDH was still used as loading control for densitometric analysis of protein levels. *$P < 0.05$.

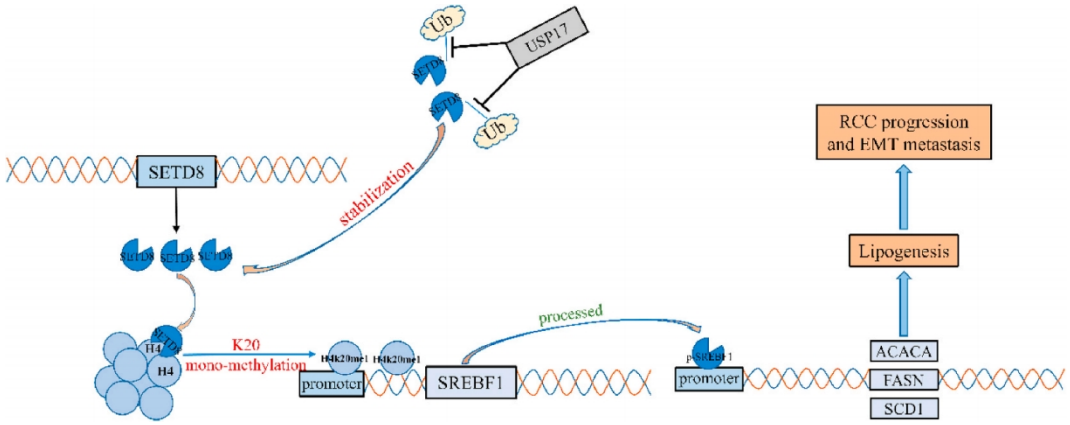

Fig. 8. A schematic diagram depicting the mechanism of SETD8 stabilized by USP17 epigenetically targeting SREBP1 to promote lipogenesis, progression and metastasis of RCC.

addition to H4K20, SETD8 can also bind or methylate other nonhistone substrates, including p53 [64], PCNA [65] and numb [66], which have been proven to play important roles in the development of cancers. However, we did not explore this issue in our present research; thus, it will be a priority in further studies.

In summary, we found that SETD8, which is stabilized by USP17, enhanced the proliferation and metastasis by advancing lipogenesis of RCC cells by epigenetically modulating the expression of the SREBP1-mediated fatty acid pathway. In this manner, SETD8 may serve as an effective biomarker for predicting prognosis and a therapeutic target inhibited by the inhibitor UNC0379 for ccRCC. Finally, these findings should render valuable implications in the biological and clinical context.

Author contribution statement

Xiaofeng Li: Conceptualization, Investigation, Writing – original draft.

Zhengfang Liu: Formal analysis, Methodology.

Chuanyou Xia and Keqiang Yan: Data curation, Resources.

Zhiqing Fang: Writing – review & editing, Project administration, Validation.

Yidong Fan: Supervision, Project administration, Revision, Funding acquisition.

Funding

This research was funded by the National Natural Science Foundation of China (Nos. 81572515, 81472395, and 81672522).

Declaration of interest statement

All authors declare that there is no conflict in the financial interest and personal relationship among them that could inappropriately influence the publication of this work.

Appendix A. Supplementary data

Supplementary data to this article can be found online at https://doi.org/10.1016/j.canlet.2021.12.018.

References

[1] F. Bray, J. Ferlay, I. Soerjomataram, R.L. Siegel, L.A. Torre, A. Jemal, Global cancer statistics 2018: GLOBOCAN estimates of incidence and mortality worldwide for 36 cancers in 185 countries, CA A Cancer J. Clin. 68 (2018) 394–424.

[2] E. Jonasch, C.L. Walker, W.K. Rathmell, Clear cell renal cell carcinoma ontogeny and mechanisms of lethality, Nat. Rev. Nephrol. 17 (2021) 245–261.

[3] S.C. Joosten, K.M. Smits, M.J. Aarts, V. Melotte, A. Koch, V.C. Tjan-Heijnen, M. van Engeland, Epigenetics in renal cell cancer: mechanisms and clinical applications, Nat. Rev. Urol. 15 (2018) 430–451.

[4] M.A. Dawson, T. Kouzarides, Cancer epigenetics: from mechanism to therapy, Cell 150 (2012) 12–27.

[5] K. Nishioka, J.C. Rice, K. Sarma, H. Erdjument-Bromage, J. Werner, Y. Wang, S. Chuikov, P. Valenzuela, P. Tempst, R. Steward, J.T. Lis, C.D. Allis, D. Reinberg, PR-Set7 is a nucleosome-specific methyltransferase that modifies lysine 20 of histone H4 and is associated with silent chromatin, Mol. Cell. 9 (2002) 1201–1213.

[6] H.A. Drabkin, R.M. Gemmill, Cholesterol and the development of clear-cell renal carcinoma, Curr. Opin. Pharmacol. 12 (2012) 742–750.

[7] Z. Zhao, Y. Liu, Q. Liu, F. Wu, X. Liu, H. Qu, Y. Yuan, J. Ge, Y. Xu, H. Wang, The mRNA expression signature and prognostic analysis of multiple fatty acid metabolic enzymes in clear cell renal cell carcinoma, J. Cancer 10 (2019) 6599–6607.

[8] L. Albiges, A.A. Hakimi, W. Xie, R.R. McKay, R. Simantov, X. Lin, J.L. Lee, B.I. Rini, S. Srinivas, G.A. Bjarnason, S. Ernst, L.A. Wood, U.N. Vaishamayan, S.Y. Rha, N. Agarwal, T. Yuasa, S.K. Pal, A. Bamias, E.C. Zabor, A.J. Skanderup, H. Furberg, A.P. Fay, G. de Velasco, M.A. Preston, K.M. Wilson, E. Cho, D.F. McDermott, S. Signoretti, D.Y.C. Heng, T.K. Choueiri, Body mass index and metastatic renal cell carcinoma: clinical and biological correlations, J. Clin. Oncol. 34 (2016) 3655–3663.

[9] K. Wakabayashi, M. Okamura, S. Tsutsumi, N.S. Nishikawa, T. Tanaka, I. Sakakibara, J. Kitakami, S. Ihara, Y. Hashimoto, T. Hamakubo, T. Kodama, H. Aburatani, J. Sakai, The peroxisome proliferator-activated receptor gamma/retinoid X receptor alpha heterodimer targets the histone modification enzyme PR-Set7/Setd8 gene and regulates adipogenesis through a positive feedback loop, Mol. Cell Biol. 29 (2009) 3544–3555.

[10] T. Liao, Y.J. Wang, J.Q. Hu, Y. Wang, L.T. Han, B. Ma, R.L. Shi, N. Qu, W.J. Wei, Q. Guan, J. Xiang, J.Y. Chen, G.H. Sun, D.S. Li, X.M. Mu, Q.H. Ji, Histone methyltransferase KMT5A gene modulates oncogenesis and lipid metabolism of papillary thyroid cancer in vitro, Oncol. Rep. 39 (2018) 2185–2192.

[11] J.L. Goldstein, R.A. DeBose-Boyd, M.S. Brown, Protein sensors for membrane sterols, Cell 124 (2006) 35–46.

[12] C. Zhou, W. Qian, J. Li, J. Ma, X. Chen, Z. Jiang, L. Cheng, W. Duan, Z. Wang, Z. Wu, Q. Ma, X. Li, High glucose microenvironment accelerates tumor growth via SREBP1-autophagy axis in pancreatic cancer, J. Exp. Clin. Cancer Res. 38 (2019) 302.

[13] N. Zhang, H. Zhang, Y. Liu, P. Su, J. Zhang, X. Wang, M. Sun, B. Chen, W. Zhao, L. Wang, H. Wang, M.S. Moran, B.G. Haffty, Q. Yang, SREBP1, targeted by miR-18a-5p, modulates epithelial-mesenchymal transition in breast cancer via forming a co-repressor complex with Snail and HDAC1/2, Cell Death Differ. 26 (2019) 843–859.

[14] L. Li, L. Hua, H. Fan, Y. He, W. Xu, L. Zhang, J. Yang, F. Deng, F. Zeng, Interplay of PKD3 with SREBP1 promotes cell growth via upregulating lipogenesis in prostate cancer cells, J. Cancer 10 (2019) 6395–6404.

[15] Y.A. Wen, X. Xiong, Y.Y. Zaytseva, D.L. Napier, E. Vallee, A.T. Li, C. Wang, H. L. Weiss, B.M. Evers, T. Gao, Downregulation of SREBP inhibits tumor growth and initiation by altering cellular metabolism in colon cancer, Cell Death Dis. 9 (2018) 265.

[16] A.A. Hakimi, E. Reznik, C.H. Lee, C.J. Creighton, A.R. Brannon, A. Luna, B. A. Aksoy, E.M. Liu, R. Shen, W. Lee, Y. Chen, S.M. Stirdivant, P. Russo, Y.B. Chen, S.K. Tickoo, V.E. Reuter, E.H. Cheng, C. Sander, J.J. Hsieh, An integrated metabolic Atlas of clear cell renal cell carcinoma, Cancer Cell 29 (2016) 104–116.

[17] D. Shen, Y. Gao, Q. Huang, Y. Xuan, Y. Yao, L. Gu, Y. Huang, Y. Zhang, P. Li, Y. Fan, L. Tang, S. Du, S. Wu, H. Wang, C. Wang, H. Gong, Y. Pang, X. Ma, B. Wang, X. Zhang, E2F1 promotes proliferation and metastasis of clear cell renal cell carcinoma via activation of SREBP1-dependent fatty acid biosynthesis, Cancer Lett. 514 (2021) 48–62.

[18] A.B. Nowakowski, W.J. Wobig, D.H. Petering, Native SDS-PAGE: high resolution electrophoretic separation of proteins with retention of native properties including bound metal ions, Metallomics 6 (2014) 1068–1078.
[19] A. Ma, W. Yu, F. Li, R.M. Bleich, J.M. Herold, K.V. Butler, J.L. Norris, V. Korboukh, A. Tripathy, W.P. Janzen, C.H. Arrowsmith, S.V. Frye, M. Vedadi, P.J. Brown, J. Jin, Discovery of a selective, substrate-competitive inhibitor of the lysine methyltransferase SETD8, J. Med. Chem. 57 (2014) 6822–6833.
[20] V. Veschi, Z. Liu, T.C. Voss, L. Ozbun, B. Gryder, C. Yan, Y. Hu, A. Ma, J. Jin, S. J. Mazur, N. Lam, B.K. Souza, G. Giannini, G.L. Hager, C.H. Arrowsmith, J. Khan, E. Appella, C.J. Thiele, Epigenetic siRNA and chemical screens identify SETD8 inhibition as a therapeutic strategy for p53 activation in high-risk neuroblastoma, Cancer Cell 31 (2017) 50–63.
[21] M. Hilvo, C. Denkert, L. Lehtinen, B. Muller, S. Brockmoller, T. Seppanen-Laakso, J. Budczies, E. Bucher, L. Yetukuri, S. Castillo, E. Berg, H. Nygren, M. Sysi-Aho, J. L. Griffin, O. Fiehn, S. Loibl, C. Richter-Ehrenstein, C. Radke, T. Hyotylainen, O. Kallioniemi, K. Iljin, M. Oresic, Novel theranostic opportunities offered by characterization of altered membrane lipid metabolism in breast cancer progression, Cancer Res. 71 (2011) 3236–3245.
[22] L. Ma, B.A. Corl, Transcriptional regulation of lipid synthesis in bovine mammary epithelial cells by sterol regulatory element binding protein-1, J. Dairy Sci. 95 (2012) 3743–3755.
[23] H.F. Xu, J. Luo, W.S. Zhao, Y.C. Yang, H.B. Tian, H.B. Shi, M. Bionaz, Overexpression of SREBP1 (sterol regulatory element binding protein 1) promotes de novo fatty acid synthesis and triacylglycerol accumulation in goat mammary epithelial cells, J. Dairy Sci. 99 (2016) 783–795.
[24] K. Fukuura, Y. Inoue, C. Miyajima, S. Watanabe, M. Tokugawa, D. Morishita, N. Ohoka, M. Komada, H. Hayashi, The ubiquitin-specific protease USP17 prevents cellular senescence by stabilizing the methyltransferase SET8 and transcriptionally repressing p21, J. Biol. Chem. 294 (2019) 16429–16439.
[25] A.P. Feinberg, B. Tycko, The history of cancer epigenetics, Nat. Rev. Cancer 4 (2004) 143–153.
[26] S.B. Baylin, P.A. Jones, A decade of exploring the cancer epigenome - biological and translational implications, Nat. Rev. Cancer 11 (2011) 726–734.
[27] Y. Gui, G. Guo, Y. Huang, X. Hu, A. Tang, S. Gao, R. Wu, C. Chen, X. Li, L. Zhou, M. He, Z. Li, X. Sun, W. Jia, J. Chen, S. Yang, F. Zhou, X. Zhao, S. Wan, R. Ye, C. Liang, Z. Liu, P. Huang, C. Liu, H. Jiang, Y. Wang, H. Zheng, L. Sun, X. Liu, Z. Jiang, D. Feng, J. Chen, S. Wu, J. Zou, Z. Zhang, R. Yang, J. Zhao, C. Xu, W. Yin, Z. Guan, J. Ye, H. Zhang, J. Li, K. Kristiansen, M.L. Nickerson, D. Theodorescu, Y. Li, X. Zhang, S. Li, J. Wang, H. Yang, J. Wang, Z. Cai, Frequent mutations of chromatin remodeling genes in transitional cell carcinoma of the bladder, Nat. Genet. 43 (2011) 875–878.
[28] K.C. Wang, H.Y. Chang, Molecular mechanisms of long noncoding RNAs, Mol. Cell. 43 (2011) 904–914.
[29] T. Kouzarides, Chromatin modifications and their function, Cell 128 (2007) 693–705.
[30] J.C. Black, C. Van Rechem, J.R. Whetstine, Histone lysine methylation dynamics: establishment, regulation, and biological impact, Mol. Cell. 48 (2012) 491–507.
[31] J. Fang, Q. Feng, C.S. Ketel, H. Wang, R. Cao, L. Xia, H. Erdjument-Bromage, P. Tempst, J.A. Simon, Y. Zhang, Purification and functional characterization of SET8, a nucleosomal histone H4-lysine 20-specific methyltransferase, Curr. Biol. 12 (2002) 1086–1099.
[32] T.S. Girish, R.K. McGinty, S. Tan, Multivalent interactions by the Set8 histone methyltransferase with its nucleosome substrate, J. Mol. Biol. 428 (2016) 1531–1543.
[33] L. Serrano, P. Martinez-Redondo, A. Marazuela-Duque, B.N. Vazquez, S.J. Dooley, P. Voigt, D.B. Beck, N. Kane-Goldsmith, Q. Tong, R.M. Rabanal, D. Fondevila, P. Munoz, M. Kruger, J.A. Tischfield, A. Vaquero, The tumor suppressor SirT2 regulates cell cycle progression and genome stability by modulating the mitotic deposition of H4K20 methylation, Genes Dev. 27 (2013) 639–653.
[34] T. Abbas, E. Shibata, J. Park, S. Jha, N. Karnani, A. Dutta, CRL4(Cdt2) regulates cell proliferation and histone gene expression by targeting PR-Set7/Set8 for degradation, Mol. Cell. 40 (2010) 9–21.
[35] D.B. Beck, H. Oda, S.S. Shen, D. Reinberg, PR-Set7 and H4K20me1: at the crossroads of genome integrity, cell cycle, chromosome condensation, and transcription, Genes Dev. 26 (2012) 325–337.
[36] S. Dulev, J. Tkach, S. Lin, N.N. Batada, SET8 methyltransferase activity during the DNA double-strand break response is required for recruitment of 53BP1, EMBO Rep. 15 (2014) 1163–1174.
[37] Z. Ma, Downregulation of SETD8 by miR-382 is involved in glioma progression, Pathol. Res. Pract. 214 (2018) 356–360.
[38] L. Piao, N. Che, H. Li, M. Li, Y. Feng, X. Liu, S. Kim, Y. Jin, Y. Xuan, SETD8 promotes stemness characteristics and is a potential prognostic biomarker of gastric adenocarcinoma, Exp. Mol. Pathol. 117 (2020) 104560.
[39] M. Liu, Y. Qin, Q. Hu, W. Liu, S. Ji, W. Xu, G. Fan, Z. Ye, Z. Zhang, X. Xu, X. Yu, Q. Zhuo, SETD8 potentiates constitutive ERK1/2 activation via epigenetically silencing DUSP10 expression in pancreatic cancer, Cancer Lett. 499 (2021) 265–278.
[40] R. Huang, Y. Yu, X. Zong, X. Li, L. Ma, Q. Zheng, Monomethyltransferase SETD8 regulates breast cancer metabolism via stabilizing hypoxia-inducible factor 1alpha, Cancer Lett. 390 (2017) 1–10.
[41] D. Hanahan, R.A. Weinberg, Hallmarks of cancer: the next generation, Cell 144 (2011) 646–674.
[42] C. Huang, C. Freter, Lipid metabolism, apoptosis and cancer therapy, Int. J. Mol. Sci. 16 (2015) 924–949.
[43] C. Cheng, F. Geng, X. Cheng, D. Guo, Lipid metabolism reprogramming and its potential targets in cancer, Cancer Commun. 38 (2018) 27.
[44] A. Nohturfft, S.C. Zhang, Coordination of lipid metabolism in membrane biogenesis, Annu. Rev. Cell Dev. Biol. 25 (2009) 539–566.
[45] J.D. Horton, J.L. Goldstein, M.S. Brown, SREBPs: activators of the complete program of cholesterol and fatty acid synthesis in the liver, J Clin Invest 109 (2002) 1125–1131.
[46] X. Hua, J. Wu, J.L. Goldstein, M.S. Brown, H.H. Hobbs, Structure of the human gene encoding sterol regulatory element binding protein-1 (SREBF1) and localization of SREBF1 and SREBF2 to chromosomes 17p11.2 and 22q13, Genomics 25 (1995) 667–673.
[47] H. Shimano, I. Shimomura, R.E. Hammer, J. Herz, J.L. Goldstein, M.S. Brown, J. D. Horton, Elevated levels of SREBP-2 and cholesterol synthesis in livers of mice homozygous for a targeted disruption of the SREBP-1 gene, J Clin Invest 100 (1997) 2115–2124.
[48] J. Yi, J. Zhu, J. Wu, C.B. Thompson, X. Jiang, Oncogenic activation of PI3K-AKT-mTOR signaling suppresses ferroptosis via SREBP-mediated lipogenesis, Proc. Natl. Acad. Sci. U. S. A. 117 (2020) 31189–31197.
[49] D. Xu, Z. Wang, Y. Xia, F. Shao, W. Xia, Y. Wei, X. Li, X. Qian, J.H. Lee, L. Du, Y. Zheng, G. Lv, J.S. Leu, H. Wang, D. Xing, T. Liang, M.C. Hung, Z. Lu, The gluconeogenic enzyme PCK1 phosphorylates INSIG1/2 for lipogenesis, Nature 580 (2020) 530–535.
[50] Y. Perone, A.J. Farrugia, A. Rodriguez-Meira, B. Gyorffy, C. Ion, A. Uggetti, A. Chronopoulos, P. Marrazzo, M. Faronato, S. Shousha, C. Davies, J.H. Steel, N. Patel, A. Del Rio Hernandez, C. Coombes, G. Pruneri, A. Lim, F. Calvo, L. Magnani, SREBP1 drives Keratin-80-dependent cytoskeletal changes and invasive behavior in endocrine-resistant ERalpha breast cancer, Nat. Commun. 10 (2019) 2115.
[51] Y. Gao, X. Nan, X. Shi, X. Mu, B. Liu, H. Zhu, B. Yao, X. Liu, T. Yang, Y. Hu, S. Liu, SREBP1 promotes the invasion of colorectal cancer accompanied upregulation of MMP7 expression and NF-kappaB pathway activation, BMC Cancer 19 (2019) 685.
[52] X. Luo, C. Cheng, Z. Tan, N. Li, M. Tang, L. Yang, Y. Cao, Emerging roles of lipid metabolism in cancer metastasis, Mol. Cancer 16 (2017) 76.
[53] H. Tanaka, S.I. Takebayashi, A. Sakamoto, T. Igata, Y. Nakatsu, N. Saitoh, S. Hino, M. Nakao, The SETD8/PR-set7 methyltransferase functions as a barrier to prevent senescence-associated metabolic remodeling, Cell Rep. 18 (2017) 2148–2161.
[54] X. Chen, X. Ding, Q. Wu, J. Qi, M. Zhu, C. Miao, Monomethyltransferase SET8 facilitates hepatocellular carcinoma growth by enhancing aerobic glycolysis, Cell Death Dis. 10 (2019) 312.
[55] Z.G. Zheng, S.T. Zhu, H.M. Cheng, X. Zhang, G. Cheng, P.M. Thu, S.P. Wang, H. J. Li, M. Ding, L. Qiang, X.W. Chen, Q. Zhong, P. Li, X. Xu, Discovery of a potent SCAP degrader that ameliorates HFD-induced obesity, hyperlipidemia and insulin resistance via an autophagy-independent lysosomal pathway, Autophagy (2020) 1–22.
[56] M. de la Vega, A.A. Kelvin, D.J. Dunican, C. McFarlane, J.F. Burrows, J. Jaworski, N.J. Stevenson, K. Dib, J.Z. Rappoport, C.J. Scott, A. Long, J.A. Johnston, The deubiquitinating enzyme USP17 is essential for GTPase subcellular localization and cell motility, Nat. Commun. 2 (2011) 259.
[57] Y. Pereg, B.Y. Liu, K.M. O'Rourke, M. Sagolla, A. Dey, L. Komuves, D.M. French, V. M. Dixit, Ubiquitin hydrolase Dub3 promotes oncogenic transformation by stabilizing Cdc25A, Nat. Cell Biol. 12 (2010) 400–406.
[58] T. Liu, J. Yu, M. Deng, Y. Yin, H. Zhang, K. Luo, B. Qin, Y. Li, C. Wu, T. Ren, Y. Han, P. Yin, J. Kim, S. Lee, J. Lin, L. Zhang, J. Zhang, S. Nowsheen, L. Wang, J. Boughey, M.P. Goetz, J. Yuan, Z. Lou, CDK4/6-dependent activation of DUB3 regulates cancer metastasis through SNAIL1, Nat. Commun. 8 (2017) 13923.
[59] Y. Wu, Y. Wang, Y. Lin, Y. Liu, Y. Wang, J. Jia, P. Singh, Y.I. Chi, C. Wang, C. Dong, W. Li, M. Tao, D. Napier, Q. Shi, J. Deng, B.M. Evers, B.P. Zhou, Dub3 inhibition suppresses breast cancer invasion and metastasis by promoting Snail1 degradation, Nat. Commun. 8 (2017) 14228.
[60] Y. Lin, Y. Wang, Q. Shi, Q. Yu, C. Liu, J. Feng, J. Deng, B.M. Evers, B.P. Zhou, Y. Wu, Stabilization of the transcription factors slug and twist by the deubiquitinase dub3 is a key requirement for tumor metastasis, Oncotarget 8 (2017) 75127–75140.
[61] C.H. Lu, D.W. Yeh, C.Y. Lai, Y.L. Liu, L.R. Huang, A.Y. Lee, S.C. Jin, T.H. Chuang, USP17 mediates macrophage-promoted inflammation and stemness in lung cancer cells by regulating TRAF2/TRAF3 complex formation, Oncogene 37 (2018) 6327–6340.
[62] X. Chen, C. Wang, K. Liao, S. Zhou, L. Cao, J. Chen, C. Xu, Y. Lin, USP17 suppresses tumorigenesis and tumor growth through deubiquitinating AEP, Int. J. Biol. Sci. 15 (2019) 738–748.
[63] C. McFarlane, A.A. Kelvin, M. de la Vega, U. Govender, C.J. Scott, J.F. Burrows, J. A. Johnston, The deubiquitinating enzyme USP17 is highly expressed in tumor biopsies, is cell cycle regulated, and is required for G1-S progression, Cancer Res. 70 (2010) 3329–3339.
[64] X. Shi, I. Kachirskaia, H. Yamaguchi, L.E. West, H. Wen, E.W. Wang, S. Dutta, E. Appella, O. Gozani, Modulation of p53 function by SET8-mediated methylation at lysine 382, Mol. Cell. 27 (2007) 636–646.
[65] M. Takawa, H.S. Cho, S. Hayami, G. Toyokawa, M. Kogure, Y. Yamane, Y. Iwai, K. Maejima, K. Ueda, A. Masuda, N. Dohmae, H.I. Field, T. Tsunoda, T. Kobayashi, T. Akasu, M. Sugiyama, S. Ohnuma, Y. Atomi, B.A. Ponder, Y. Nakamura, R. Hamamoto, Histone lysine methyltransferase SETD8 promotes carcinogenesis by deregulating PCNA expression, Cancer Res. 72 (2012) 3217–3227.
[66] G.K. Dhami, H. Liu, M. Galka, C. Voss, R. Wei, K. Muranko, T. Kaneko, S.P. Cregan, L. Li, S.S. Li, Dynamic methylation of Numb by Set8 regulates its binding to p53 and apoptosis, Mol. Cell. 50 (2013) 565–576.